Regnase-1 deficiency restrains *Klebsiella pneumoniae* infection by regulation of a Type I interferon response

Running title: Loss of Regnase-1 promotes resilience to *Klebsiella pneumoniae*

Giraldina Trevejo-Nuñez[a#], Becky Lin[a], Li Fan[b], Felix E. Y. Aggor[c], Partha S. Biswas[c], Kong Chen[b], and Sarah L. Gaffen[c]

[a]Division of Infectious Diseases, University of Pittsburgh School of Medicine, Pittsburgh, Pennsylvania, USA

[b]Division of Pulmonary, Allergy and Critical Care Medicine, University of Pittsburgh School of Medicine, Pittsburgh, Pennsylvania, USA

[c]Division of Rheumatology and Clinical Immunology, University of Pittsburgh School of Medicine, Pittsburgh, Pennsylvania, USA

[#]Corresponding author: Giraldina Trevejo-Nuñez, MD

giraldina.trevejo@pitt.edu

Abstract

Excessive inflammatory responses can cause collateral tissue damage or autoimmune inflammation, sometimes with severe morbidity or mortality. During host defense responses, numerous negative feedback mechanisms are established to prevent excessive unchecked inflammation. However, this restraint can sometimes come at the cost of suboptimal infection control, and we do not fully understand how this balance is maintained during different infection settings. The endoribonuclease Regnase-1 (Reg1, *Zc3h12a*, MCPIP1) is an RNA binding protein (RBP) that binds and degrades many target mRNA transcripts. Reg1 is a potent feedback regulator of IL-17 and LPS signal transduction, among other stimuli. Consequently, Reg1 deficiency exacerbates autoimmune inflammation in multiple mouse models, but on the other hand, reduced Reg1 improves immunity to fungal infection. To date, the role of Reg1 in bacterial immunity is poorly defined. Here, we show that mice deficient in Reg1 are more resistant to pulmonary *Klebsiella pneumoniae* (KP) infection. Unexpectedly, effects of Reg1 deficiency were not due to accelerated eradication of bacteria or increased pro-inflammatory cytokine expression. Rather, alveolar macrophages from Reg1-deficient mice showed enrichment of Type I IFN-related genes upon KP infection, accompanied by increased *Ifnb1* expression. Surprisingly, the stability of *Ifnb1* was not altered by Reg1-deficiency; rather, mRNA encoding its upstream regulator IRF7 appeared to be a more prominent target. Thus, impaired Reg1 induces Type I IFN and enhances resistance to KP, raising the possibility that Reg1 could be a potential clinical target in acute bacterial infections.

Introduction

Klebsiella pneumoniae (KP) is part of the normal human microbiome and is detected in approximately 10% of the Human Microbiome Project samples (1, 2). KP is the third most common cause of ventilator-associated pneumonia (VAP) in the US, and its presence correlates with prolonged duration of ventilation and ICU hospital stay (3-5). KP imposes a major infectious disease challenge due to increasing antimicrobial resistance and comparatively limited therapeutic options (6). Hence, an improved understanding of host-pathogen interactions is needed to elucidate, and ultimately exploit, the host mechanisms that control KP pneumonia.

The immune response to infectious pathogens is finely balanced to allow eradication of microbes yet still prevent excessive inflammatory pathology. Thus, numerous mechanisms are triggered during immune responses to counter-regulate excessive or unnecessary responses and minimize collateral damage to the host. The RNA-binding protein Regnase-1 (Reg1), also known as MCP1-induced protein 1 (MCPIP1), is encoded by the *ZC3H12A* gene and has intrinsic endoribonuclease activity that keeps inflammatory responses in check (7). Reg1 degrades target gene transcripts, including its own mRNA, through recognition of characteristic stem-loop secondary structures in the 3' untranslated region (UTR) of target mRNAs (8). Reg1 is induced by many inflammatory stimuli, including IL-1, Toll-like-receptors (TLR) and IL-17 (9-12). In addition, TCR signaling leads to cleavage of Reg1, releasing T cells from Reg1-mediated suppression (13). Thus, Reg1 plays a central role in driving of pro-inflammatory cytokines through post-transcriptional control of RNA longevity.

Multiple mouse models support the vital role of Reg1 as a negative regulator of pathogenic inflammation. Reg1 knockout (*Zc3h12a*$^{-/-}$, here called *Reg1*$^{-/-}$) mice have a life span only of 6-8 weeks. *Reg1*$^{-/-}$ mice display significant constitutive inflammation, manifesting as

growth retardation, splenomegaly, lymphadenopathy, heightened systemic and localized cytokine production, and multi-organ failure (9, 14). To avoid confounding issues with the complete knockout, we have frequently taken advantage of *Reg1* heterozygous mice (*Reg1*$^{+/-}$), which have normal life spans and fertility, normal tonic expression of Reg1, and minimal peripheral organ inflammation at baseline (11, 15). Even so, cells from *Reg1*$^{+/-}$ mice display markedly reduced Reg1 expression after LPS or IL-17 stimulation, and tissues from *Reg1*$^{+/-}$ animals (lung, kidney, CNS) exhibit elevated cytokine responses (11). Consequently, *Reg1*$^{+/-}$ mice show exacerbated signs of autoimmunity in multiple IL-17-driven autoimmune conditions, including experimental autoimmune encephalomyelitis (EAE), imiquimod (IMQ)-induced dermatitis and autoantibody-induced glomerulonephritis (AGN). In all these settings, IL-17R deficiency reversed the phenotype, demonstrating that Reg1 functions in these settings through restricting IL-17-driven inflammation (11, 15, 16).

In contrast to exacerbating pathology in autoimmune conditions, Reg1-deficiency led to improved resistance to an IL-17-mediated host response, disseminated candidiasis, causing enhanced survival and concomitantly reduced fungal kidney burdens (11). Therefore, although restraint of Reg1 is clearly beneficial to limit autoimmune pathology, it is conceivable that temporary blockade of Reg1 could be exploited to improve IL-17-driven immune responses during certain infectious settings. However, the impact of Reg1 in infectious disease settings has not been extensively explored.

KP is recognized in the host by pattern recognition receptors such as TLR4, which activates the myeloid differentiation primary response gene 88 (MyD88)- dependent pathway leading to induction of pro-inflammatory chemokines and cytokines. TLR4 signaling also induces the TIR-domain-containing adaptor-inducing interferon -β (TRIF) pathway which leads

to induction of Type I IFN (IFN-α and IFN-β). Both TLR4 signaling pathways are needed for defense against KP infection (17, 18). TLR4 is upstream of IL-17 production from γδ T cells in response to KP (19), and *Il17ra*$^{-/-}$ mice have uncontrolled KP infection with decreased expression of CXC chemokines, G-CSF and impaired neutrophil recruitment (20). Additionally, IL-17 synergizes with cytokines such as IL-22 to increase production of antimicrobial peptides in lung epithelium, such as LCN2, S100A, MUC1, CXCL5 (21). Though produced by lymphocytes, IL-17 mediates downstream signals selectively on non-hematopoietic cells in the pulmonary epithelium during KP infection (22). Thus, TLR4 and IL-17R pathways mediated an integrated inflammatory cascade that contains KP lung infection.

Given the documented role of Reg1 in restricting both TRL4- and IL-17-dependent host responses, we hypothesized that Reg1-deficiency would be protective in the context of KP pneumonia, likely through decreased mRNA decay of pro-inflammatory transcripts. Indeed, Reg1-deficiency rendered mice resistant to KP. However, bacterial burdens and typical pro-inflammatory cytokines known to be targeted by Reg1 were not altered in Reg1-deficent mice. Gene profiling of sorted alveolar macrophages of KP- infected mice showed enrichment of type I IFN-associated gene pathways during Reg1 deficiency. We found that Reg1 regulates the stability of the mRNA encoding IRF7, an upstream regulator of Type 1 IFN gene expression by TLRs.

Material and Methods

Mice

Reg1$^{+/-}$ and *Reg1*$^{+/+}$ *(Zc3h12a)* littermates on the C57BL/6 background were co-housed and used for all experiments. *Reg1(Zc3h12a)*$^{fl/fl}$ mice are under material transfer agreement (MTA) from University of Central Florida (Orlando, Florida, USA). *Sftpc*^{Cre} mice and CD45.1 mice were from The Jackson Laboratory. Mice were 8-12-weeks old and both sexes were used. All animal studies were approved by the Institutional Animal Care and Use Committee (IACUC) of the University of Pittsburgh.

Bacterial infections

KP ATCC strain 43816 was grown in tryptic soy broth to reach early log phase. 1-2x10^3 CFU/mouse in PBS was administered by deep oropharyngeal aspiration. Where indicated, tamoxifen (TAM) was administered i.p. at 75 mg/kg dissolved in corn oil for 5 d and then rested for 5 d prior to induction of infection.

Bone marrow chimeras

WT (CD45.1) and *Reg1*$^{+/-}$ (CD45.2) mice were lethally irradiated (900 Gy). After 24h, each mouse received 4x10^6 bone marrow cells by tail vein injection. Mice received antibiotics in drinking water starting 1 d before irradiation and continued for 10 d (trimethroprim/sulfametoxazole 200/40 mg). After 6 weeks, engraftment was confirmed by flow cytometry of blood for CD45.1 and CD45.2 markers.

Bacterial burden, mRNA, and protein analysis

Tissues were homogenized in PBS and CFU levels were assessed by serial dilution plating. Lung tissues were homogenized in TrIzol (Invitrogen) and subjected to qPCR with SybrGreen probes. Threshold cycle (C_T) values were normalized to *Gapdh*. ELISA kits were from eBioscience (Thermo Fisher Scientific) and R&D Systems. Abs used for western blots were cleaved caspase-3, total caspase 3 (Cell signaling) and beta-actin (Abcam).

Flow cytometry

Lungs were digested with lung dissociation kits (Miltenyi). Lung cell suspensions were stained for CD45, LyG, CD11b, CD11c, SiglecF, Ly6C, CD3, CD4, NK1.1, IFN-γ. Antibodies were from eBioscience, BD Biosciences or Biolegend. Alveolar macrophages ($CD45^+$, LyG^- $CD11b^-$ $CD11c^{hi}$, $SiglecF^+$) were sorted by flow cytometry. Proliferation was assessed by BrDU incorporation (BD Biosciences); briefly, mice were injected intraperitoneally with 1 mg of BrDU one day before sacrifice. Data were acquired on LSR Fortessa and analyzed with FlowJo software.

Bone marrow derived macrophages (BMDM)

BM cells were extracted from *Reg1*$^{+/-}$ and *Reg1*$^{+/+}$ mice femur and tibia and differentiated into BMDM with L929 media (30%) for 5-6 days. Cultured BMDMs were stimulated with heat-killed KP (MOI of 10) up to 8 hours or *Klebsiella* LPS (1ug/ml) (Sigma-Aldrich).

RNA Sequencing and Analysis

Reg1$^{+/-}$ and *Reg1*$^{+/+}$ littermate control mice were infected with KP by oropharyngeal aspiration. After 24 h, alveolar macrophages were stained as described above and sorted by flow cytometry. Cells were placed directly into RLT-plus (Qiagen, Valencia, CA) and total cellular RNA was extracted using the RNeasy MiniKit (Qiagen). RNA was quantitated using Nanodrop, and integrity was determined with a total RNA Nano Chip (Agilent Technologies). Single-stranded total RNA-seq libraries were sequenced with an Illumina Nextseq500 sequencer with a depth of 25 million reads per sample (75 bp single-end) at the University of Pittsburgh Health Sciences Sequencing Core. Fastq files with high quality reads (phred score >30) were uploaded to the CLC Genomics Workbench (Qiagen) and reads aligned to the mouse reference genome. Transcript counts and differential expression analyses were carried out using the CLC Genomics Workbench.

Statistical Analysis

Data were analyzed on Prism (GraphPad). Data were analyzed by Log-Rank, One-way analysis of variance (ANOVA), Student's t test, and post hoc tests were used as indicated. Each symbol represents one mouse unless indicated.

Results

Reg1-deficient mice are resistant to KP lung infection

A complete absence of Reg1 is extremely deleterious for the host, as Reg1$^{-/-}$ mice exhibit severe inflammation and severely shortened life spans (9). In contrast, *Reg1*$^{+/-}$ mice (somtimes termed Reg1-deficient) have a normal life span without peripheral organ inflammation, yet show enhanced pro-inflammatory responses in multiple IL-17-driven autoinflammatory model settings (11, 15, 16). To determine whether Reg1 haploinsufficiency influences immunity to KP infection, *Reg1*$^{+/-}$ and *Reg1*$^{+/+}$ littermate controls were infected with KP by oropharyngeal aspiration. Survival and parameters of health including weight loss were monitored over time. Indeed, infection-induced survival and weight loss were significantly ameliorated in Reg1-deficient mice compared to *Reg1*$^{+/+}$ littermate controls (**Fig. 1A, B**). Unexpectedly, this improvement in survival was not accompanied by statistically significant differences in lung bacterial burdens (**Fig 1C**). Moreover, there were no differences in bacterial dissemination into the spleen between groups at any measured time point (**Fig. 1D**), even though that *Reg1*$^{+/-}$ mice had lower expression of Reg1 (*Zc3h12a*) than control mice **(Fig. 1E).** These data suggest that factors other than bacterial burden underlie the improved survival in Reg1-deficient hosts.

Reg1 functions in both hematopoietic and non-hematopoietic compartments during KP pneumonia

Reg1 has been shown to act in multiple cell types, including T cells, macrophages and epithelial cells (7, 23). Of relevance to KP, Reg1 can restrict signaling by both TLR4 and IL-17. Whereas TLR4 acts predominantly on hematopoietic cells (especially macrophages), IL-

17 mediates signals in epithelial and/or mesenchymal target tissues, including lung (24). Therefore, to define the essential compartments in which Reg1 functions to limit immunity to pulmonary KP infection, we used an adoptive transfer approach. Femoral bone marrow cells from *Reg1*$^{+/-}$ (CD45.2) and WT (CD45.1) mice were transferred into irradiated *Reg1*$^{+/-}$ or WT recipients. After 8 weeks, engraftment was assessed by flow cytometry (data not shown). Successfully reconstituted mice were infected with KP by oropharyngeal aspiration and followed up to 7 days. As expected, WT mice that received WT BM cells were susceptible to KP, whereas *Reg1*$^{+/-}$ mice receiving *Reg1*$^{+/-}$ BM were more resistant. As shown, *Reg1*$^{+/-}$ or WT mice that received *Reg1*$^{+/-}$ BM cells were resistant to KP, with almost 80% survival at day 7 post-infection. Additionally, *Reg1*$^{+/-}$ mice that received WT BM cells were resistant to KP, showing 60% survival at day 7 (**Fig 2A**). Thus, Reg1 appears to act in multiple compartments.

Loss of IL-17RA in pulmonary epithelial cells renders mice highly susceptible to KP infection (24). Accordingly, given the potent impact of Reg1 on IL-17 signaling seen in prior studies (11, 12, 15, 25), we crossed *Reg1*$^{fl/fl}$ mice to Surfactant protein C (*Sftpc*)^{Cre} mice in order to delete Reg1 conditionally in distal epithelial cells (distal bronchi and alveoli). As shown, mice were modestly more resistant to KP than controls, but the improvement survival was much less profound than seen in *Reg1*$^{+/-}$ mice (**Fig 2B**), which is consistent with the bone marrow chimera data showing contributions from both the hematopoietic and non-hematopoietic compartments contribute upon KP infection.

Reg1 deficiency does not influence immune cell recruitment or proliferation during KP infection

Based on these data, Reg1 deficiency in the hematopoietic compartment provides a survival advantage to the host. However, we saw no changes in recruitment of myeloid cells between *Reg1*$^{+/-}$ and control mice at 48 h and 72 h post-infection (**Fig 3A**). Consistent with this, expression of myeloid-recruiting chemokines such as *Cxcl1*, *Cxcl5* and *Ccl2* were similar among groups, despite the fact that these are all known transcriptional targets of Reg1 in other settings (**Fig. S1A**) (26, 27). There were also no differences in cellular proliferation and macrophage bacterial killing between *Reg1*$^{+/-}$ and control mice (**Fig 3B, C**). It is known that Reg1 controls B cell homeostasis and that complete Reg1 deletion in B cells increases antibody secretion (28). However, IgM and IgA levels in BALF and lung tissue were comparable between *Reg1*$^{+/-}$ and control mice (**Fig 3D**). Taken together, these data suggest that differences in survival during KP infection in *Reg1*$^{+/-}$ mice is not explained by altered recruitment of myeloid cells, cellular proliferation, macrophage killing capacity, or a B cell antibody response.

Resistance to KP caused by Reg1 deficiency is linked to increased interferon (IFN) signature

To understand the mechanisms by which Reg1 deficiency promotes survival, we performed transcriptomic profiling of purified alveolar macrophages from *Reg1*$^{+/-}$ and littermate control lungs at 24 h post-KP infection. This time point was chosen to define the early events that are operative during the initial stages of infection. There were 796

differentially expressed genes, of which 237 were upregulated and 559 were downregulated. Gene set enrichment analysis (GSEA) revealed major changes in type I IFN-related responses (IFN-α), oxidative phosphorylation, and IFN-γ response as the top three enriched gene sets, with a normalized enrichment score (NES) <2.5 for the type I IFN group (**Fig. 4A, B**).

We next validated these pathways by functional analysis. Consistent with the RNASeq data, Type I IFN (IFN-β) expression was higher in lung homogenates of Reg1-deficient mice compared to controls at 24 h and 48 h post-infection **(Fig 5A**). Since IFN-β can be produced by macrophages during Gram-negative pneumonia (29), we stimulated *Reg1*$^{+/-}$ or control BMDMs with heat-killed KP and assessed *Ifnb1* mRNA. Indeed, *Ifnb1* was elevated in Reg1-deficient macrophages compared to controls as early as 2 h post-infection (**Fig. 5B**). In contrast, IFN-γ expression was similarly expressed between *Reg1*$^{+/-}$ and Reg1$^{+/+}$ mice after KP infection (**Fig 5C**). Similarly, oxidative phosphorylation, of sorted alveolar macrophages assessed by mitochondrial respiration, was not different between *Reg1*$^{+/-}$ mice and controls (**Fig. S1B,C**). Collectively, these data indicate that Reg1 deficiency induces IFN-β upon KP infection.

Reg1 is as an RBP that promotes endonucleolytic decay of target transcripts (30). Based on the observed increased *Ifnb1* expression in Reg-deficient BMDMs, we hypothesized that Reg1 deficiency may result in prolonged stabilization of *Ifnb1* mRNA or regulatory factors upstream of *Ifnb1* regulation. To test this, *Reg1*$^{+/-}$ and control BMDMs were stimulated with LPS to prime expression of genes in the IFN pathway. Cells were treated with actinomycin D (Act D) to block further transcription, and the half-life of candidate target transcripts was assessed over a 2-hour time course. Although the intrinsic mRNA stability of *Ifnb1* or other mRNAs was not detectably altered in Reg1-deficient cells, the half-life of *Irf7*

mRNA considerably increased in the setting of Reg1 deficiency (**Fig. 5D**), potentially explaining the increased IFN-β seen in Reg-1 deficient mice upon KP pneumonia.

Increased Ifnb1 correlates with enhanced anti-inflammatory response in Reg1-deficient mice

IFN-β has the capacity to exert anti-inflammatory effects in the host, reported in several disease models. This effect has been attributed in part to type I IFN induction of IL-10, which dampens expression of transcription of cytokines such as *Tnfa, Cxcl1, Il6* (31, 32). Based on this, we assessed IL-10 in lung homogenates of KP-infected mice. There was a trend to increased IL-10 at 72 h post-infection in *Reg1*$^{+/-}$ mice compared to control mice, though this did not reach statistical significance (**Fig 6A**). TNF-α was not affected *Reg1*$^{+/-}$ compared to controls (**Fig 6B**). We then asked whether apoptosis was affected in *Reg1*$^{+/-}$ mice compared to controls. As shown, cleaved caspase 3 expression in total lung homogenates was increased in *Reg1* $^{+/-}$ mice compared to controls (**Fig 6C, D**). These data suggest that increased IFN-β arising from Reg1 deficiency may confer an anti-inflammatory advantage to *Reg1*$^{+/-}$ mice sufficient to prolong survival upon KP infection.

Discussion

Reg1 controls the inflammatory response by degrading many individual inflammatory cytokine mRNAs, including *Il6, Il1b,* and *Il12b,* thus tempering the overall inflammatory milieu (9). Perhaps even more significantly, Reg1 degrades transcripts encoding inflammatory transcription factors (TF) such as *Nfkbiz,* which encodes the non-canonical TF IκBξ, and therefore Reg1 can indirectly affect all IκBξ-inducible genes (11). Thus, it is not surprising that a complete knockout of Reg1 gene (*Zc3h12a*) is fatal in animals due to severe autoinflammation. *Reg1*$^{+/-}$ mice, on the other hand, have a normal life span and do not exhibit peripheral baseline inflammation. However, *Reg1*$^{+/-}$ mice still have an enhanced inflammatory response, particularly when the disease model relies heavily on the IL-17R pathway (11, 15, 25). In this KP infection model, we were surprised that levels of inflammatory cytokines and chemokines were similar between Reg1-deficient mice and controls. Since these mice are haploinsufficient for the Reg1 gene (*Zc3h12a*), and KP is initially recognized by TLR4, one potential explanation is the remaining Reg1 levels may be enough to compensate for the cytoplasmicMyD88-driven pathway, but not the endosomal TRIF-dependent pathway, thus leading to increased type I IFN expression and protection from KP.

The role of type I interferons (IFN-α/IFN-β) in bacterial infections is still not fully defined, especially when compared to its extensively-studied roles in viral infections. Even among bacterial pathogens, the response to type I IFN differs depending on site of infection and pathogen characteristics. For instance, type I IFN is detrimental in animal models of *Staphylococcus aureus* and *Listeria monocytogenes* (33, 34). On the other hand, there is a protective response in models of *Legionella pneumophilia* and *Streptococcus pyogenes (35).* In the case of *Klebsiella pneumoniae,* IFN-β signaling in NK cells enhances secretion of IFN-γ,

decreasing bacterial burden (36). In this study, we did not see differences in recruitment of NK cells or enhanced IFN-γ secretion by NK cells in *Reg1*$^{+/-}$ mice compared to controls. However, the enhanced mortality in control WT mice is significantly decreased in *Reg1*$^{+/-}$ mice, which we propose is due to increased type I IFN that modulates the inflammatory response enough to facilitate bacterial eradication and pneumonia resolution.

IFN-β leads to increased apoptosis, macrophage efferocytosis and resolution of infection in models of *E. coli* pneumonia and peritonitis, associated with enhanced IL-10 secretion (29). IL-10 mediates many anti-inflammatory effects and regulates metabolic reprograming of macrophages (37). Although there was only a modest trend of increased IL-10, there was a clear increase in cleaved Caspase-3 in Reg1-deficient lungs, correlating with increased IFN-β and resistance to KP pneumonia. Concomitantly, transcriptomic profiles revealed several IFN-stimulated genes (ISGs) involved in apoptosis, including *Ifit2, Ifit3* and *Ifitm3*. Intriguingly, IFIT2 is an RBP known to enhance apoptosis (38, 39), though its precise role in the context of Reg1 immunoregulation is as yet unknown. Since IFN-β was increased in Reg1- deficient mice upon KP infection, we initially expected that Reg1 deficiency would result in enhanced stability of the *Ifnb1* transcript. However, our data instead suggested that the impact on *Ifnb1* is likely indirect via control of *Irf7* mRNA, opening a new view of how Reg1 influences immune responses.

The immune system has evolved to balance the vital effects of anti-microbial effector functions with the potential for causing collateral tissue damage. In this regard, the activation of every immune signaling pathway is accompanied by negative feedback signaling events that restrain inflammation (40, 41). In selected conditions, however, it may be clinically beneficial to allow more fulminant inflammation in order to treat a life-threatening condition. Indeed,

checkpoint inhibitor blockade for cancer therapy is built on exploiting this concept (42). By analogy, releasing inflammatory “brakes” may be useful in the context of severe infections such as bacterial pneumonia, and the present data suggest that Reg1 could, in principle at least, be one such target.

Acknowledgements

GTN was supported by NIH grants HL135476, HL154231, AI153549. KC was supported by HL137709. SLG was supported by AI147383. We thank BM Coleman for technical support and JK Kolls for helpful discussions.

Abbreviations: BM, bone marrow; BMDM, bone marrow-derived macrophages; KP, *Klebsiella pneumoniae*; MCPIP1, MCP1-induced protein 1 (alternative name for Regnase-1); MyD88, myeloid differentiation primary response gene 88; RBP, RNA binding protein; Reg1, regnase-1; TAM, tamoxifen; TLR, Toll-like receptor; UTR, untranslated region; VAP, ventilator-associated pneumonia

Author contributions

Conceptualization – GTN, PSB, SLG, KC

Investigation – GTN, BL, LF, FEYA

Writing – GTN, SLG

Reviewing and Editing – GTN, KC, PSB, SLG

Visualization – GTN

Supervision – GTN, SLG, PSB

Funding Acquisition – GTN, SLG, KC, PBS

References

1. Conlan, S., H. H. Kong, and J. A. Segre. 2012. Species-level analysis of DNA sequence data from the NIH Human Microbiome Project. *PLoS One* 7: e47075.
2. Martin, R. M., J. Cao, S. Brisse, V. Passet, W. Wu, L. Zhao, P. N. Malani, K. Rao, and M. A. Bachman. 2016. Molecular Epidemiology of Colonizing and Infecting Isolates of Klebsiella pneumoniae. *mSphere* 1: e00261-00216.
3. Papazian, L., M. Klompas, and C. E. Luyt. 2020. Ventilator-associated pneumonia in adults: a narrative review. *Intensive Care Med* 46: 888-906.
4. Weiner, L. M., A. K. Webb, B. Limbago, M. A. Dudeck, J. Patel, A. J. Kallen, J. R. Edwards, and D. M. Sievert. 2016. Antimicrobial-Resistant Pathogens Associated With Healthcare-Associated Infections: Summary of Data Reported to the National Healthcare Safety Network at the Centers for Disease Control and Prevention, 2011-2014. *Infect Control Hosp Epidemiol* 37: 1288-1301.
5. Gorrie, C. L., M. Mirceta, R. R. Wick, D. J. Edwards, N. R. Thomson, R. A. Strugnell, N. F. Pratt, J. S. Garlick, K. M. Watson, D. V. Pilcher, S. A. McGloughlin, D. W. Spelman, A. W. J. Jenney, and K. E. Holt. 2017. Gastrointestinal Carriage Is a Major Reservoir of Klebsiella pneumoniae Infection in Intensive Care Patients. *Clin Infect Dis* 65: 208-215.
6. Adler, A., D. E. Katz, and D. Marchaim. 2020. The Continuing Plague of Extended-Spectrum β-Lactamase Producing Enterbacterales Infections: An Update. *Infect Dis Clin North Am* 34: 677-708.
7. Fu, M., and P. J. Blackshear. 2017. RNA-binding proteins in immune regulation: a focus on CCCH zinc finger proteins. *Nat Rev Immunol* 17: 130-143.

8. Mino, T., Y. Murakawa, A. Fukao, A. Vandenbon, H. H. Wessels, D. Ori, T. Uehata, S. Tartey, S. Akira, Y. Suzuki, C. G. Vinuesa, U. Ohler, D. M. Standley, M. Landthaler, T. Fujiwara, and O. Takeuchi. 2015. Regnase-1 and Roquin Regulate a Common Element in Inflammatory mRNAs by Spatiotemporally Distinct Mechanisms. *Cell* 161: 1058-1073.

9. Matsushita, K., O. Takeuchi, D. M. Standley, Y. Kumagai, T. Kawagoe, T. Miyake, T. Satoh, H. Kato, T. Tsujimura, H. Nakamura, and S. Akira. 2009. Zc3h12a is an RNase essential for controlling immune responses by regulating mRNA decay. *Nature* 458: 1185-1190.

10. Iwasaki, H., O. Takeuchi, S. Teraguchi, K. Matsushita, T. Uehata, K. Kuniyoshi, T. Satoh, T. Saitoh, M. Matsushita, D. M. Standley, and S. Akira. 2011. The IκB kinase complex regulates the stability of cytokine-encoding mRNA induced by TLR-IL-1R by controlling degradation of regnase-1. *Nat Immunol* 12: 1167-1175.

11. Garg, A. V., N. Amatya, K. Chen, J. A. Cruz, P. Grover, N. Whibley, H. R. Conti, G. Hernandez Mir, T. Sirakova, E. C. Childs, T. E. Smithgall, P. S. Biswas, J. K. Kolls, M. J. McGeachy, P. E. Kolattukudy, and S. L. Gaffen. 2015. MCPIP1 Endoribonuclease Activity Negatively Regulates Interleukin-17-Mediated Signaling and Inflammation. *Immunity* 43: 475-487.

12. Tanaka, H., Y. Arima, D. Kamimura, Y. Tanaka, N. Takahashi, T. Uehata, K. Maeda, T. Satoh, M. Murakami, and S. Akira. 2019. Phosphorylation-dependent Regnase-1 release from endoplasmic reticulum is critical in IL-17 response. *The Journal of experimental medicine* 216: 1431-1449.

13. Uehata, T., H. Iwasaki, A. Vandenbon, K. Matsushita, E. Hernandez-Cuellar, K. Kuniyoshi, T. Satoh, T. Mino, Y. Suzuki, D. M. Standley, T. Tsujimura, H. Rakugi, Y.

Isaka, O. Takeuchi, and S. Akira. 2013. Malt1-Induced Cleavage of Regnase-1 in CD4(+) Helper T Cells Regulates Immune Activation. *Cell* 153: 1036-1049.

14. Miao, R., S. Huang, Z. Zhou, T. Quinn, B. Van Treeck, T. Nayyar, D. Dim, Z. Jiang, C. J. Papasian, Y. Eugene Chen, G. Liu, and M. Fu. 2013. Targeted disruption of MCPIP1/Zc3h12a results in fatal inflammatory disease. *Immunol Cell Biol* 91: 368-376.

15. Monin, L., J. E. Gudjonsson, E. E. Childs, N. Amatya, X. Xing, A. H. Verma, B. M. Coleman, A. V. Garg, M. Killeen, A. Mathers, N. L. Ward, and S. L. Gaffen. 2017. MCPIP1/Regnase-1 Restricts IL-17A- and IL-17C-Dependent Skin Inflammation. *J Immunol* 198: 767-775.

16. Li, D.-D., R. Bechara, K. Ramani, C. V. Jawale, Y. Li, J. K. Kolls, S. L. Gaffen, and P. S. Biswas. 2021. RTEC-intrinsic IL-17–driven inflammatory circuit amplifies antibody-induced glomerulonephritis and is constrained by Regnase-1. *JCI Insight* 6: e147505.

17. Cai, S., S. Batra, L. Shen, N. Wakamatsu, and S. Jeyaseelan. 2009. Both TRIF- and MyD88-dependent signaling contribute to host defense against pulmonary Klebsiella infection. *J Immunol* 183: 6629-6638.

18. van Lieshout, M. H., D. C. Blok, C. W. Wieland, A. F. de Vos, C. van 't Veer, and T. van der Poll. 2012. Differential roles of MyD88 and TRIF in hematopoietic and resident cells during murine gram-negative pneumonia. *J Infect Dis* 206: 1415-1423.

19. Happel, K. I., M. Zheng, E. Young, L. J. Quinton, E. Lockhart, A. J. Ramsay, J. E. Shellito, J. R. Schurr, G. J. Bagby, S. Nelson, and J. K. Kolls. 2003. Cutting edge: roles of Toll-like receptor 4 and IL-23 in IL-17 expression in response to Klebsiella pneumoniae infection. *J Immunol* 170: 4432-4436.

20. Ye, P., F. H. Rodriguez, S. Kanaly, K. L. Stocking, J. Schurr, P. Schwarzenberger, P. Oliver, W. Huang, P. Zhang, J. Zhang, J. E. Shellito, G. J. Bagby, S. Nelson, K. Charrier, J. J. Peschon, and J. K. Kolls. 2001. Requirement of interleukin 17 receptor signaling for lung CXC chemokine and granulocyte colony-stimulating factor expression, neutrophil recruitment, and host defense. *J Exp Med* 194: 519-527.

21. Aujla, S. J., Y. R. Chan, M. Zheng, M. Fei, D. J. Askew, D. A. Pociask, T. A. Reinhart, F. McAllister, J. Edeal, K. Gaus, S. Husain, J. L. Kreindler, P. J. Dubin, J. M. Pilewski, M. M. Myerburg, C. A. Mason, Y. Iwakura, and J. K. Kolls. 2008. IL-22 mediates mucosal host defense against Gram-negative bacterial pneumonia. *Nature medicine* 14: 275-281.

22. Chen, K., T. Eddens, G. Trevejo-Nunez, E. E. Way, W. Elsegeiny, D. M. Ricks, A. V. Garg, C. J. Erb, M. Bo, T. Wang, W. Chen, J. S. Lee, S. L. Gaffen, and J. K. Kolls. 2016. IL-17 Receptor Signaling in the Lung Epithelium Is Required for Mucosal Chemokine Gradients and Pulmonary Host Defense against K. pneumoniae. *Cell Host Microbe* 20: 596-605.

23. Yang, C., S. Huang, X. Wang, and Y. Gu. 2015. Emerging Roles of CCCH-Type Zinc Finger Proteins in Destabilizing mRNA Encoding Inflammatory Factors and Regulating Immune Responses. *Crit Rev Eukaryot Gene Expr* 25: 77-89.

24. Chen, K., T. Eddens, G. Trevejo-Nunez, E. Way, W. Elsegeiny, D. Ricks, A. Garg, C. Erb, M. Bo, T. Wang, W. Chen, J. Lee, S. L. Gaffen, and J. Kolls. 2016. IL-17 Receptor Signaling in the Lung Epithelium Is Required for Mucosal Chemokine Gradients and Pulmonary Host Defense against K. pneumoniae. *Cell Host Microbe* 20: 596-605.

25. Jeltsch, K. M., D. Hu, S. Brenner, J. Zoller, G. A. Heinz, D. Nagel, K. U. Vogel, N. Rehage, S. C. Warth, S. L. Edelmann, R. Gloury, N. Martin, C. Lohs, M. Lech, J. E. Stehklein, A. Geerlof, E. Kremmer, A. Weber, H. J. Anders, I. Schmitz, M. Schmidt-Supprian, M. Fu, H. Holtmann, D. Krappmann, J. Ruland, A. Kallies, M. Heikenwalder, and V. Heissmeyer. 2014. Cleavage of roquin and regnase-1 by the paracaspase MALT1 releases their cooperatively repressed targets to promote T(H)17 differentiation. *Nature immunology* 15: 1079-1089.

26. Mino, T., Y. Murakawa, A. Fukao, A. Vandenbon, H. H. Wessels, D. Ori, T. Uehata, S. Tartey, S. Akira, Y. Suzuki, C. G. Vinuesa, U. Ohler, D. M. Standley, M. Landthaler, T. Fujiwara, and O. Takeuchi. 2015. Regnase-1 and Roquin Regulate a Common Element in Inflammatory mRNAs by Spatiotemporally Distinct Mechanisms. *Cell* 161: 1058-1073.

27. Akaki, K., K. Ogata, Y. Yamauchi, N. Iwai, K. M. Tse, F. Hia, A. Mochizuki, Y. Ishihama, T. Mino, and O. Takeuchi. 2021. IRAK1-dependent Regnase-1-14-3-3 complex formation controls Regnase-1-mediated mRNA decay. *Elife* 10.

28. Bhat, N., R. Virgen-Slane, P. Ramezani-Rad, C. R. Leung, C. Chen, D. Balsells, A. Shukla, E. Kao, J. R. Apgar, M. Fu, C. F. Ware, and R. C. Rickert. 2021. Regnase-1 is essential for B cell homeostasis to prevent immunopathology. *J Exp Med* 218: e20200971.

29. Kumaran Satyanarayanan, S., D. El Kebir, S. Soboh, S. Butenko, M. Sekheri, J. Saadi, N. Peled, S. Assi, A. Othman, S. Schif-Zuck, Y. Feuermann, D. Barkan, N. Sher, J. G. Filep, and A. Ariel. 2019. IFN-β is a macrophage-derived effector cytokine facilitating the resolution of bacterial inflammation. *Nat Commun* 10: 3471.

30. Akira, S. 2013. Regnase-1, a Ribonuclease Involved in the Regulation of Immune Responses. *Cold Spring Harb Symp Quant Biol* 78: 51-60.

31. Katakura, K., J. Lee, D. Rachmilewitz, G. Li, L. Eckmann, and E. Raz. 2005. Toll-like receptor 9-induced type I IFN protects mice from experimental colitis. *J Clin Invest* 115: 695-702.

32. Hamana, A., Y. Takahashi, A. Tanioka, M. Nishikawa, and Y. Takakura. 2018. Safe and effective interferon-beta gene therapy for the treatment of multiple sclerosis by regulating biological activity through the design of interferon-beta-galectin-9 fusion proteins. *Int J Pharm* 536: 310-317.

33. Carrero, J. A., B. Calderon, and E. R. Unanue. 2004. Type I interferon sensitizes lymphocytes to apoptosis and reduces resistance to Listeria infection. *J Exp Med* 200: 535-540.

34. Martin, F. J., M. I. Gomez, D. M. Wetzel, G. Memmi, M. O'Seaghdha, G. Soong, C. Schindler, and A. Prince. 2009. Staphylococcus aureus activates type I IFN signaling in mice and humans through the Xr repeated sequences of protein A. *J Clin Invest* 119: 1931-1939.

35. Boxx, G. M., and G. Cheng. 2016. The Roles of Type I Interferon in Bacterial Infection. *Cell Host Microbe* 19: 760-769.

36. Ivin, M., A. Dumigan, F. N. de Vasconcelos, F. Ebner, M. Borroni, A. Kavirayani, K. N. Przybyszewska, R. J. Ingram, S. Lienenklaus, U. Kalinke, D. Stoiber, J. A. Bengoechea, and P. Kovarik. 2017. Natural killer cell-intrinsic type I IFN signaling controls Klebsiella pneumoniae growth during lung infection. *PLoS Pathog* 13: e1006696.

37. Ip, W. K. E., N. Hoshi, D. S. Shouval, S. Snapper, and R. Medzhitov. 2017. Anti-inflammatory effect of IL-10 mediated by metabolic reprogramming of macrophages. *Science* 356: 513-519.

38. Reich, N. C. 2013. A death-promoting role for ISG54/IFIT2. *J Interferon Cytokine Res* 33: 199-205.

39. Yang, Z., H. Liang, Q. Zhou, Y. Li, H. Chen, W. Ye, D. Chen, J. Fleming, H. Shu, and Y. Liu. 2012. Crystal structure of ISG54 reveals a novel RNA binding structure and potential functional mechanisms. *Cell Res* 22: 1328-1338.

40. Carpenter, S., E. P. Ricci, B. C. Mercier, M. J. Moore, and K. A. Fitzgerald. 2014. Post-transcriptional regulation of gene expression in innate immunity. *Nat Rev Immunol* 14: 361-376.

41. Li, X., R. Bechara, J. Zhao, M. J. McGeachy, and S. L. Gaffen. 2019. IL-17 receptor-based signaling and implications for disease. *Nat Immunol* 20: 1594-1602.

42. Sharma, P., and J. P. Allison. 2020. Dissecting the mechanisms of immune checkpoint therapy. *Nat Rev Immunol* 20: 75-76.

43. Amatya, N., C. EE, J. A. Cruz, F. Aggor, A. Garg, A. Berman, J. E. Gudjonsson, U. Atasoy, and S. L. Gaffen. 2018. IL-17 integrates multiple self-reinforcing, feed-forward mechanisms through the RNA-binding protein Arid5a. *Science Signaling* 11: eaat4617.

Figure legends

Figure 1: Reg1-haploinsufficient mice are resistant to KP lung infection. A) Lung and B) spleen bacterial burdens were assessed by CFU assessment at the indicated time points. Each symbol represents 1 mouse. Filled circle = *Reg1*$^{+/+}$ and open box= *Reg1*$^{+/-}$ mice. C) Weight loss was assessed at the indicated time points (n=15 mice/group). D) Survival of *Reg1*$^{+/-}$ or *Reg1*$^{+/+}$ littermates was assessed up to 8 days post-infection (n=15 mice/group). E) Reg1 gene expression (*Zc3h12a*) in lung homogenates of KP-infected mice. Data are pooled from two experiments. * P<0.05, **<0.01, Log-Rank test.

Figure 2: Reg1 deficiency in both hematopoietic and non-hematopoietic compartments contribute to prolonged survival upon KP lung infection. A) *Reg1*$^{+/-}$ and *Reg1*$^{+/+}$ littermates were irradiated to ablate bone marrow (BM) and later reconstituted with reciprocal femoral BM cells. Eight weeks after BM transfer, mice were infected with KP and survival monitored over 7 days. B) *Reg1*$^{fl/fl}$ were crossed to *Sftpc*^{CreERT2} infected with KP and monitored over 7 d. Data are pooled from two experiments. * P<0.05, **<0.01, Log-Rank test.

Figure 3: Immune cell recruitment, proliferation and antibody production are not affected by Reg1 deficiency during KP infection. A) Recruitment and B) BrDU incorporation of lung myeloid cell populations were assessed by flow cytometry at baseline (0 h) or 48 and 72 h post-infection. C) Macrophage killing and Ab production in lung was

assessed at the indicated time points. Data are pooled from two experiments. Data analyzed by ANOVA and found to be non-significant.

Figure 4: RNASeq of sorted alveolar macrophages reveals an enriched Type 1 IFN gene signature. *Reg1*$^{+/-}$ and *Reg1*$^{+/+}$ littermates were infected with KP or PBS by oropharyngeal aspiration. Alveolar macrophages were sorted by flow cytometry at 24 h post infection and subjected to RNASeq. A) Gene set enrichment analysis (GSEA) of type I IFN genesets. B) Heatmap depicting differentially expressed genes in the type I IFN pathway (n=4 mice/group).

Figure 5: Increased IFN-β but not IFN-γ in Reg1 deficient mice during KP infection. *Reg1*$^{+/-}$ and *Reg1*$^{+/+}$ littermates were infected with KP. A) IFN-β was assessed in lung homogenates by ELISA. B) *Ifnb1* mRNA was assessed in cultured BMDMs infected with heat-killed KP for the indicated time points. C) Levels of IFN-γ were assessed by intracellular staining in total CD45^{+}, NK1.1^{+} and CD4^{+} cells. B) Each symbol represents one mouse. *P<0.05 One-way ANOVA with post-hoc Tukey's test. D) BMDMs were pretreated with LPS for 3 h and treated with Act D to stop new transcription. Expression of the indicated mRNAs were assessed for the indicated times by qPCR, normalized to *Gapdh*. Levels compared to time = 0 data are presented as means ± SEM, representative of 2 independent experiments. One-way ANOVA with post hoc Tukey's test *P < 0.05 by; RNA half-life ($t_{½}$) was determined by linear regression as described (43).

Figure 6: Reg1 deficiency enhances the inflammatory response and increases apoptosis. A, B) IL-10 and TFNα were assessed by ELISA in lung homogenates of the indicated mice infected

with KP. C) *Reg1*$^{+/-}$ and *Reg1*$^{+/+}$ littermates were infected with KP. Mice were sacrificed at 48h post-infection, and cleaved Caspase 3 and total Caspase were assessed in lung homogenates by immunoblotting. At right, quantified band intensity values ± SEM is shown.

Figure S1: Expression of chemokines and mitochondrial respiration is similar between Reg1$^{+/-}$ **and controls**. *Reg 1*$^{+/-}$ and *Reg1*$^{+/+}$ littermates were given PB or KP by oropharyngeal aspiration and sacrificed at 24h. A) *Cxcl1*, *Cxcl5* and *Ccl2* expression was measured in lung tissue. Data analyzed by Student t-test and found non-significant B) CD11c^{+} cells sorted from PBS-treated or C) KP- infected mice were sorted and evaluated for oxygen consumption rate (OCR) by Seahorse flux analyzer (n=4 mice per group). Data analyzed by ANOVA and found to be non-significant.

Figure 1

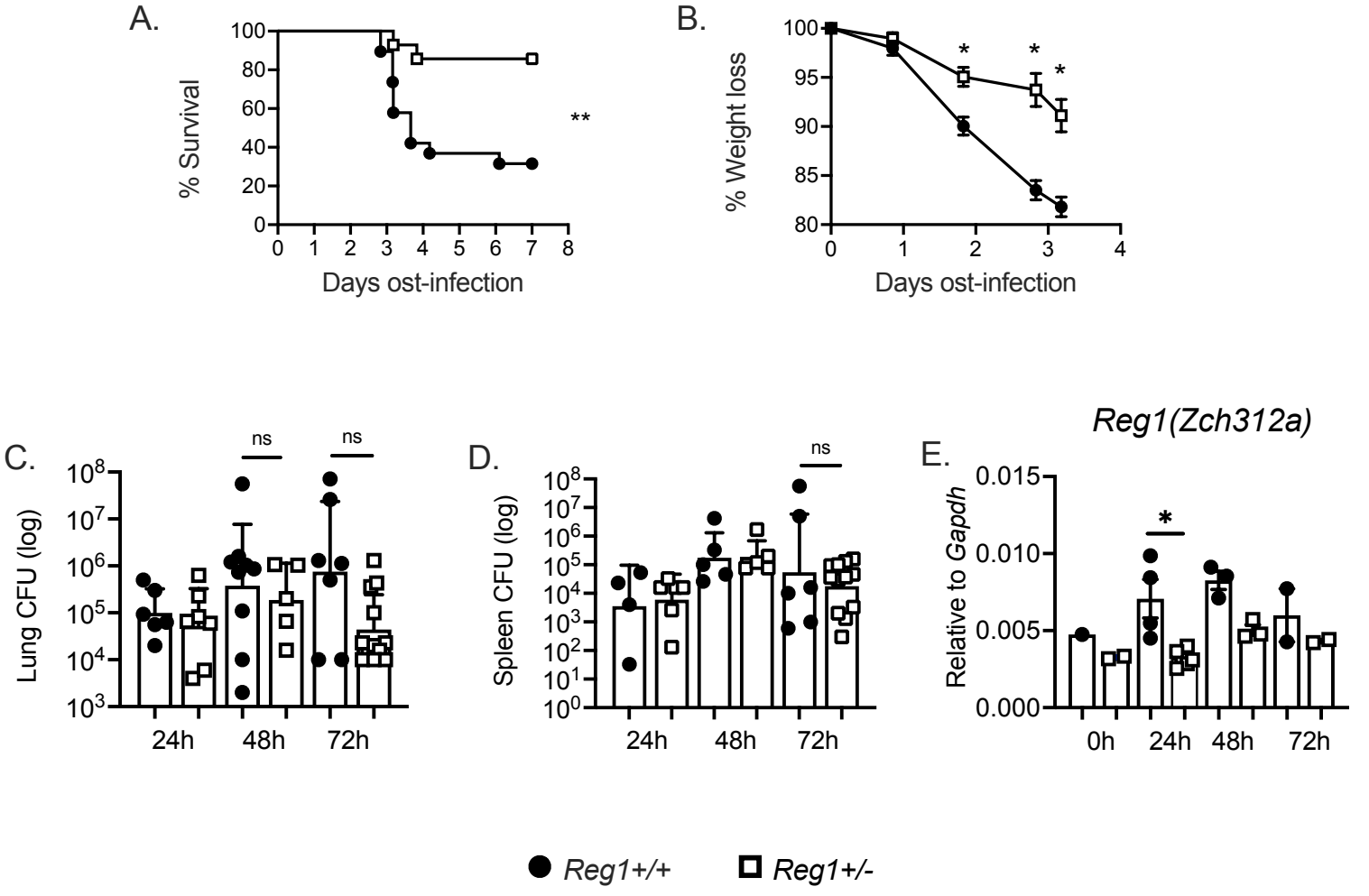
A.
% Survival
Days ost-infection
**
B.
% Weight loss
Days ost-infection
*
*
*
C.
Lung CFU (log)
ns
ns
24h
48h
72h
D.
Spleen CFU (log)
ns
24h
48h
72h
E.
Reg1(Zch312a)
Relative to Gapdh
*
0h
24h
48h
72h
Reg1+/+
Reg1+/-

Figure 2

A.

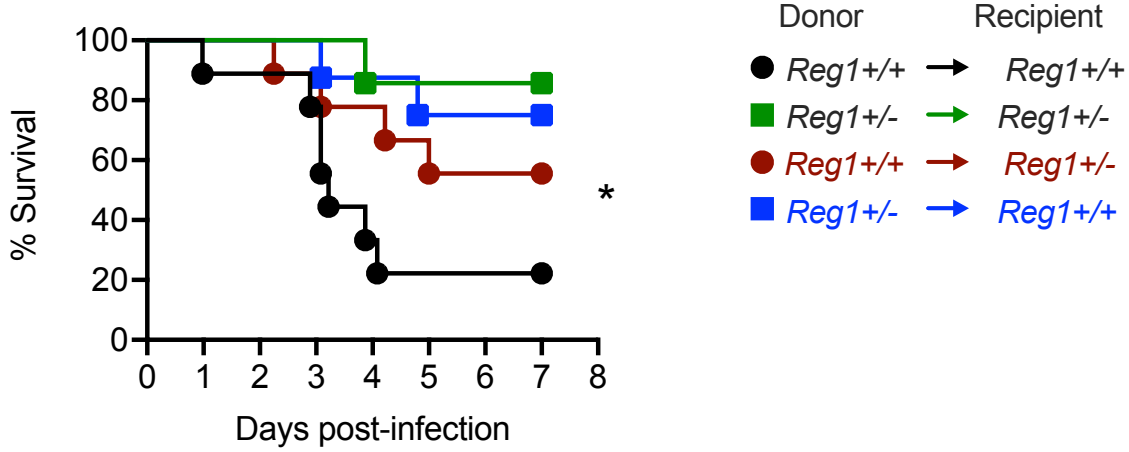
% Survival
100
80
60
40
20
0
0 1 2 3 4 5 6 7 8
Days post-infection
*
Donor
Recipient
Reg1+/+ → Reg1+/+
Reg1+/- → Reg1+/-
Reg1+/+ → Reg1+/-
Reg1+/- → Reg1+/+

B.

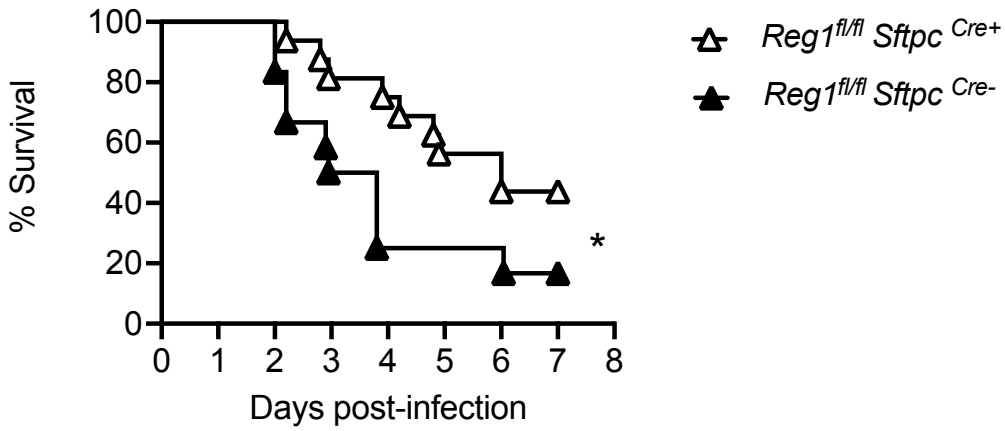
% Survival
100
80
60
40
20
0
0 1 2 3 4 5 6 7 8
Days post-infection
*
Reg1fl/fl Sftpc Cre+
Reg1fl/fl Sftpc Cre-

Figure 3

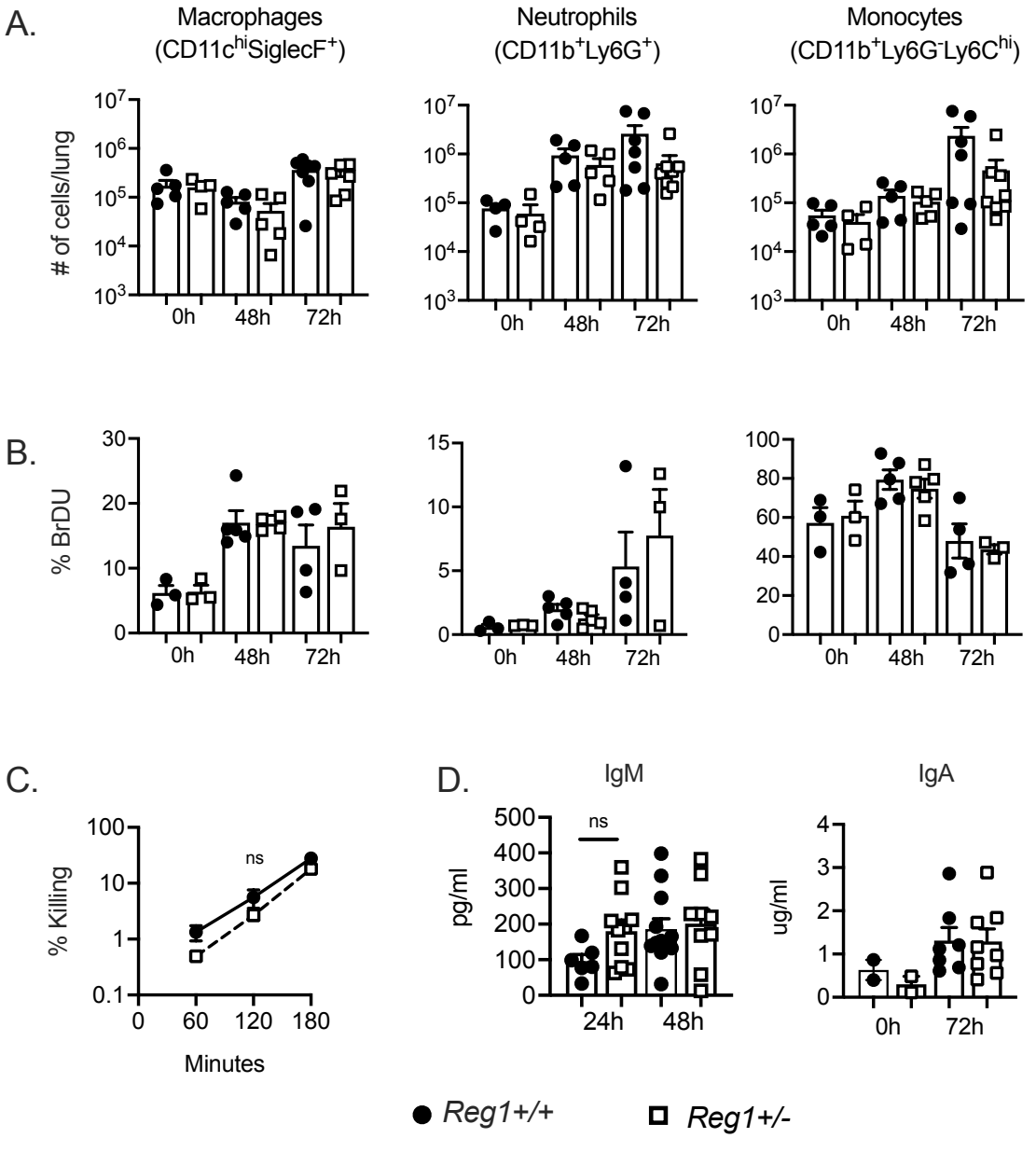
A.
Macrophages
(CD11c^hiSiglecF^+)
Neutrophils
(CD11b^+Ly6G^+)
Monocytes
(CD11b^+Ly6G^-Ly6C^hi)
# of cells/lung
0h
48h
72h
B.
% BrDU
C.
% Killing
ns
Minutes
D.
IgM
IgA
pg/ml
ug/ml
24h
Reg1+/+
Reg1+/-

Figure 4

A.

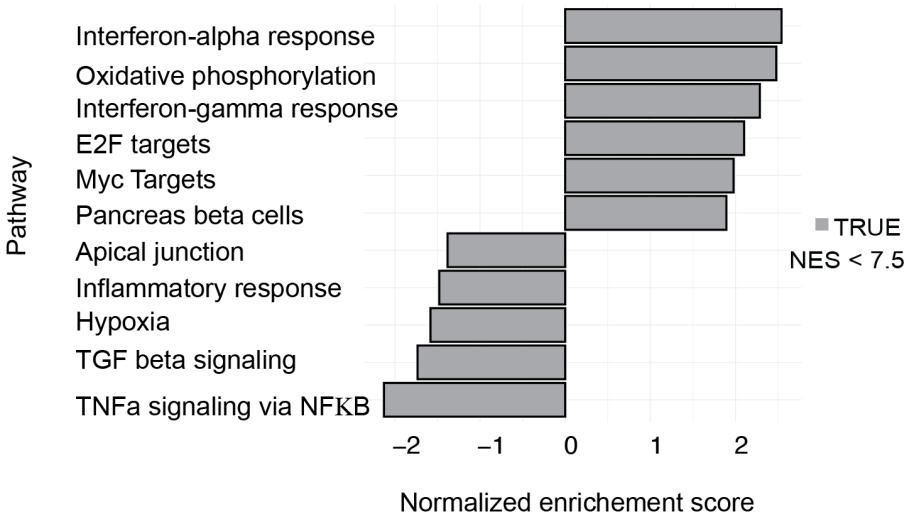
Interferon-alpha response
Oxidative phosphorylation
Interferon-gamma response
E2F targets
Myc Targets
Pancreas beta cells
Apical junction
Inflammatory response
Hypoxia
TGF beta signaling
TNFa signaling via NFKB
Pathway
TRUE
NES < 7.5
−2
−1
0
1
2
Normalized enrichement score

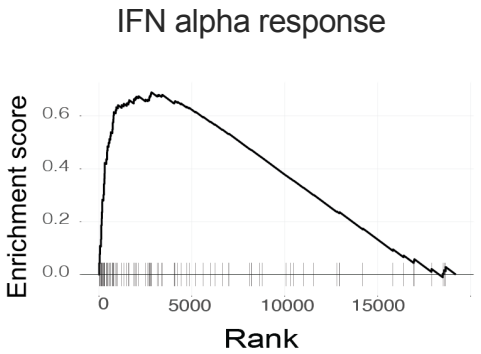
IFN alpha response
Enrichment score
0.6
0.4
0.2
0.0
0
5000
10000
15000
Rank

B.

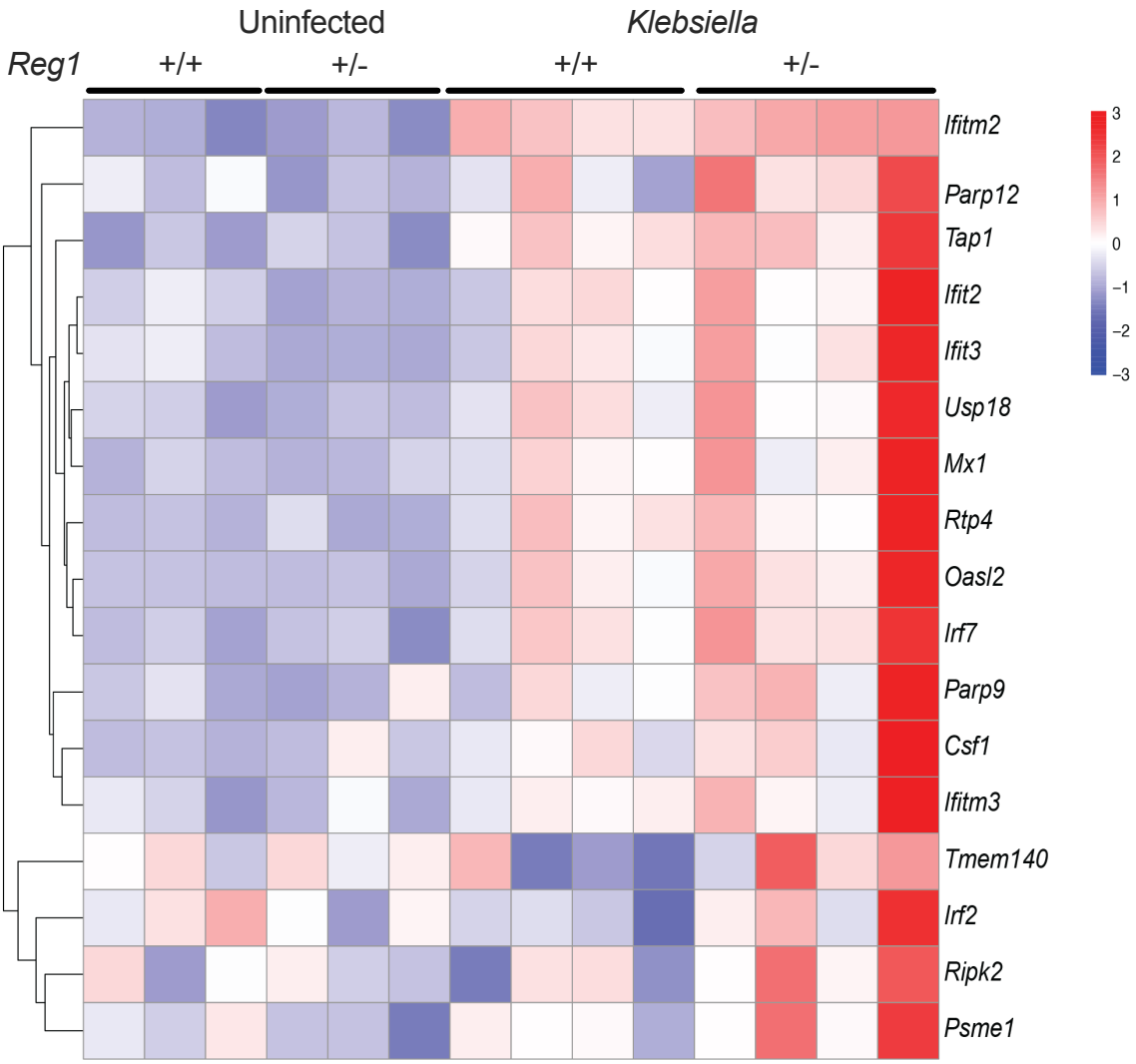
Uninfected
Klebsiella
Reg1
+/+
+/-
+/+
+/-
Ifitm2
Parp12
Tap1
Ifit2
Ifit3
Usp18
Mx1
Rtp4
Oasl2
Irf7
Parp9
Csf1
Ifitm3
Tmem140
Irf2
Ripk2
Psme1
3
2
1
0
−1
−2
−3

Figure 5

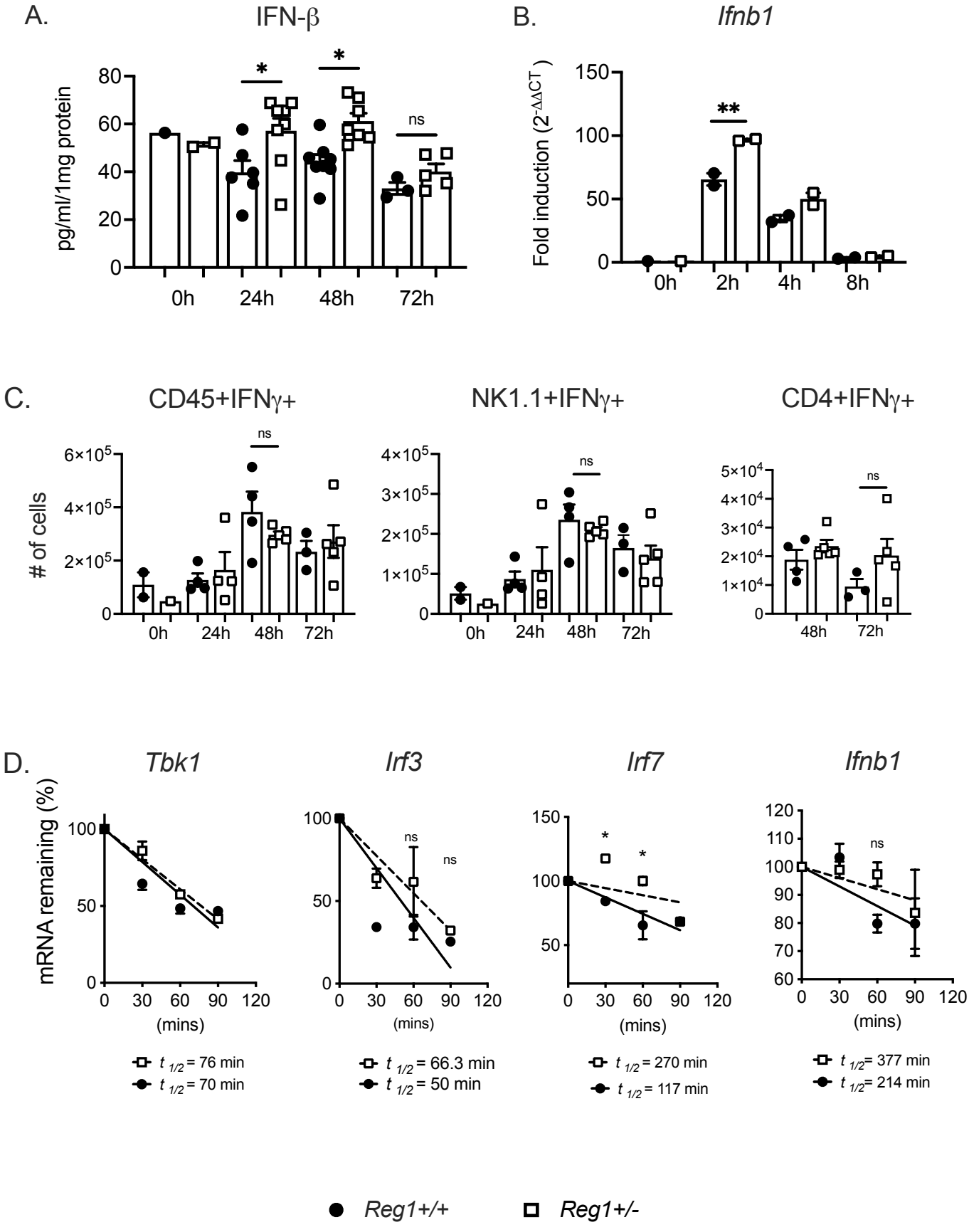
A.
IFN-β
pg/ml/1mg protein
80
60
40
20
0
*
*
ns
0h
24h
48h
72h
B.
Ifnb1
Fold induction (2^-ΔΔCT)
150
100
50
0
**
0h
2h
4h
8h
C.
CD45+IFNγ+
NK1.1+IFNγ+
CD4+IFNγ+
# of cells
6×10^5
4×10^5
2×10^5
0
4×10^5
3×10^5
2×10^5
1×10^5
5×10^4
4×10^4
3×10^4
2×10^4
1×10^4
ns
0h
24h
48h
72h
D.
Tbk1
Irf3
Irf7
Ifnb1
mRNA remaining (%)
(mins)
t 1/2 = 76 min
t 1/2 = 70 min
t 1/2 = 66.3 min
t 1/2 = 50 min
t 1/2 = 270 min
t 1/2 = 117 min
t 1/2 = 377 min
t 1/2 = 214 min
Reg1+/+
Reg1+/-

Figure 6

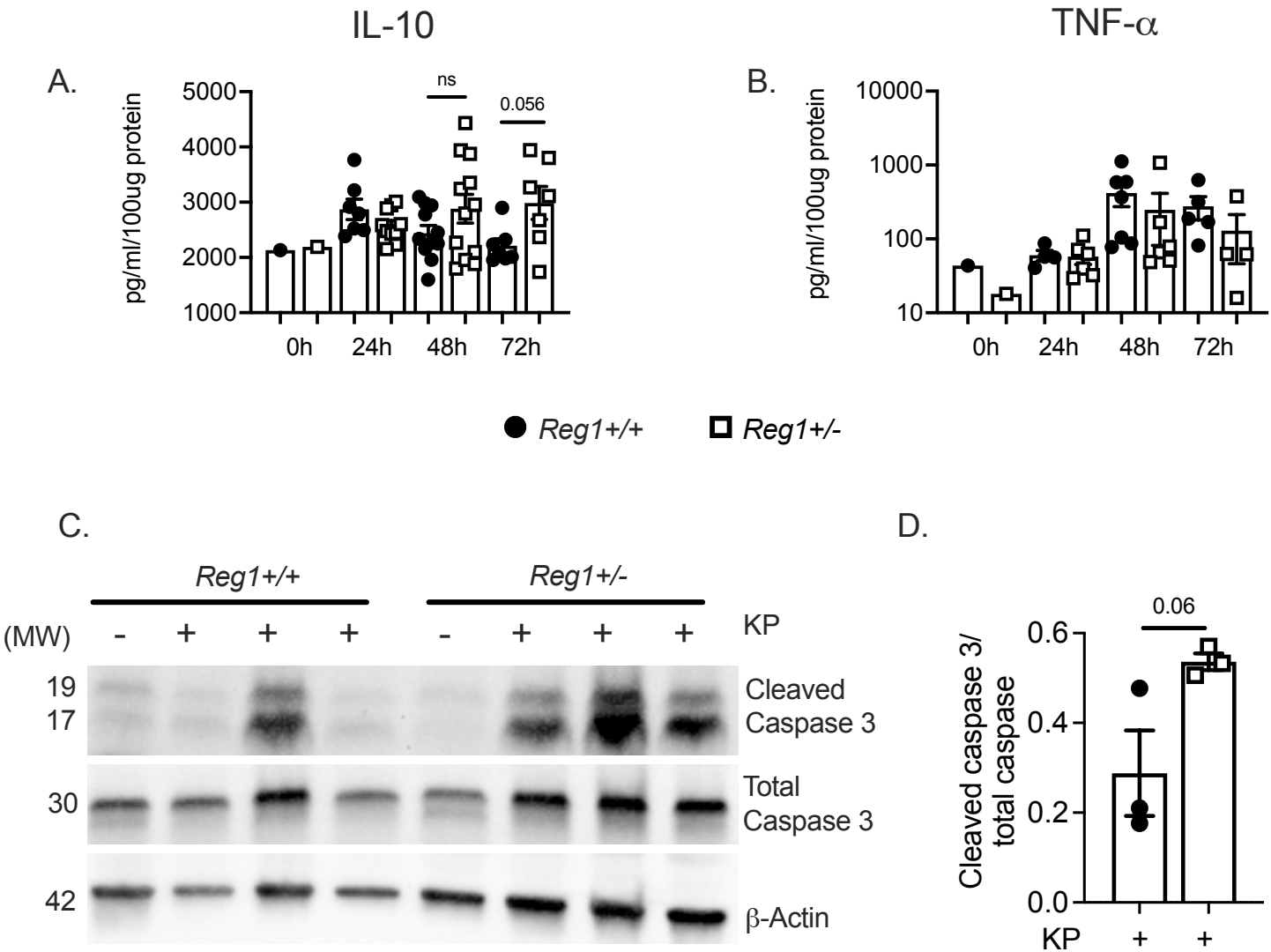
IL-10
A.
pg/ml/100ug protein
5000
4000
3000
2000
1000
ns
0.056
0h
24h
48h
72h
TNF-α
B.
pg/ml/100ug protein
10000
1000
100
10
0h
24h
48h
72h
Reg1+/+
Reg1+/-
C.
Reg1+/+
Reg1+/-
(MW)
- + + +
- + + +
KP
19
17
Cleaved Caspase 3
30
Total Caspase 3
42
β-Actin
D.
0.06
Cleaved caspase 3/ total caspase
0.6
0.4
0.2
0.0
KP
+
+
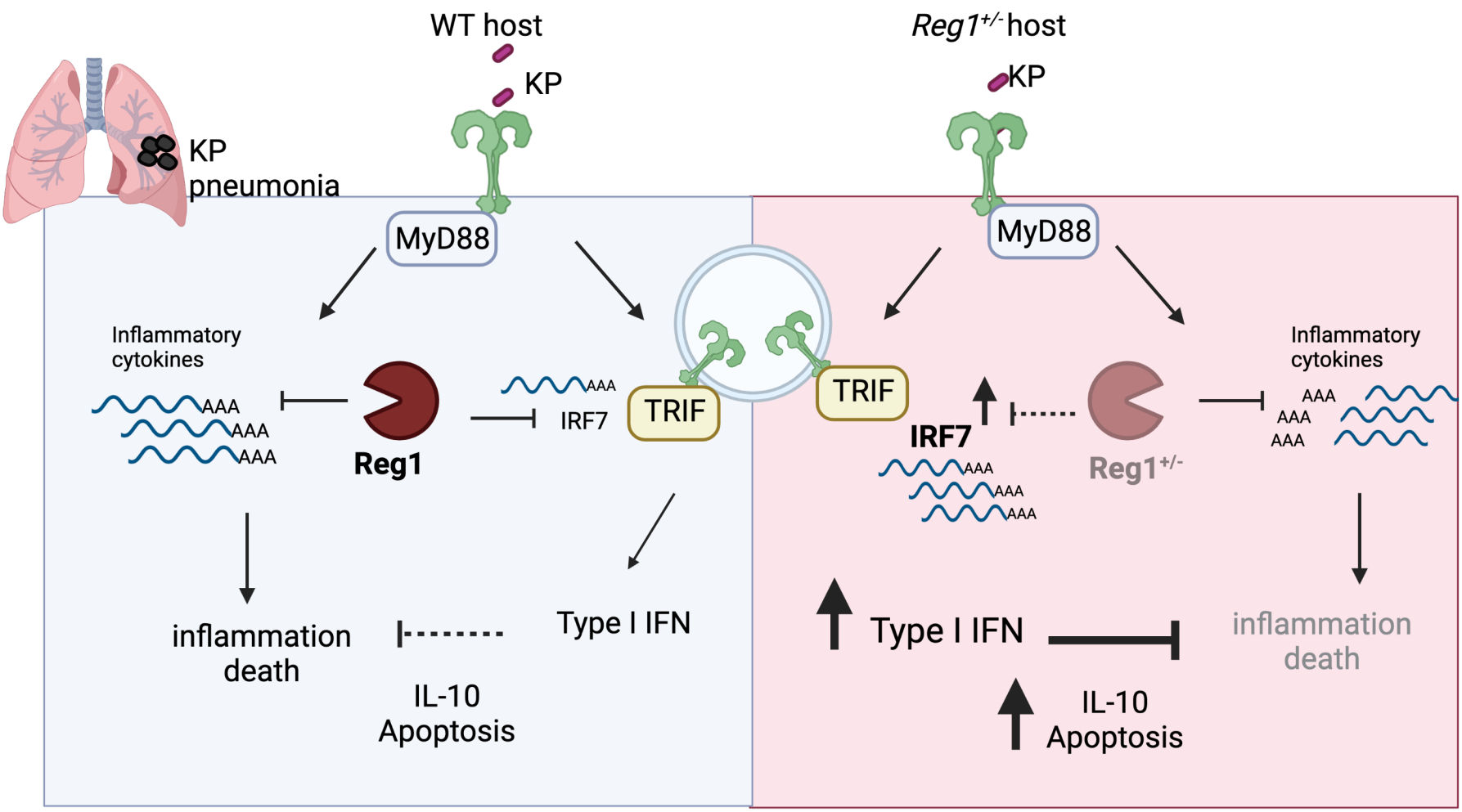
Graphical abstract